GMR
The Original

INFLUENCE OF FERRITE NANOPARTICLE ON MAGNETIC AND MECHANICAL PROPERTIES OF POLYURETHANE/POLYSTYRENE INTERPENETRATING POLYMER NETWORK

Nitin Kumar[1*], Nitika Choudhary[2], Sunil K. Dwivedi[3], Sunil Kumar[4]

[*1]Research scholar at Shri Jagdishprasad Jhabarmal Tibrewala University, Jhunjhunu, Rajasthan -333001.
[2]Ass. Prof. at Shri Jagdishprasad Jhabarmal Tibrewala University, Jhunjhunu, Rajasthan -333001
[3]Department of Physics, SAS, OM Sterling Global University, Hisar-125001
[4]Department of Physics, RR BAWA DAV College, Batala, Punjab-143505
*Corresponding Author: gorsiyanitin98@gmail.com

ABSTRACT
Thin flexible mats of $NiFe_2O_4$ incorporated PU/PS IPN has been successfully prepared using In-situ polymerization of PU/PS & $NiFe_2O_4$ using chain initiator and catalyst. X-ray diffraction peaks corresponding to spinel crystal phase (F d 3m No. 227) in non-crystalline interpenetrating polymer network reveals presence of $NiFe_2O_4$ in matrix of PU/PS. FTIR bond also endorsed X-ray diffraction data means presence of $NiFe_2O_4$ in matrix of non-crystalline PU/PS IPN. Change in rate of wt% loss with incorporation of $NiFe_2O_4$ shows improvement in thermal stability whereas elongation at break evident for enhancement in mechanical properties of PU/PS IPN. M-H magnetic hysteresis reveals establishment of magnetic behavior in non-magnetic PU/PS IPN by incorporation of $NiFe_2O_4$ in matrix of IPN. The elements present in thin flexible mat have been confirmed from energy of X-ray generated during X-ray dispersive spectroscopy whereas elemental mapping shows distribution of various elements in flexible mats. The ε', ε" & $\square_{ac}$ vs. Frequency reveals increased in dielectric properties of IPN by incorporation of $NiFe_2O_4$ during in-situ polymerization of PU/PS IPN.

KEYWORDS: Flexible Mats, Interpenetrating Polymer Network (IPN), Elongation at break, Thermal Stability, Castor Oil

INTRODUCTION

Vegetable oils, which include castor, soybean, palm, and rapeseed oils, are derived mainly from seeds of oilseed plants are used in a wide range of products, including plasticizers, meals, paints, cosmetics, medicines, and biofuels. They are also desirable monomers for polymer chemistry because of their reactive nature and natural abundance. However, because of their varied and heterogeneous architectures, use them as monomers is difficult. Indeed, because oils are usually expressed in low concentrations and because composition of a given oil can fluctuate seasonally, it can be costly to separate and extract the various triglycerides present. Recent breakthroughs in genetic engineering have signaled a breakthrough; for instance, the amount of oleic acid in variant sunflower oil. One of the most significant groups of polymers are polyurethanes (PUs), which have a wide range of uses and characteristics that can include thermosetting plastics and linear polymers. The volume fractions of soft and hard segments & chemical compositions of these segments, distribution of each segment, and degree of cross-linking are some of numerous variables that affect structural-property relationships in PU made them important in various applications. By altering components as well as stoichiometric balance affects physical, chemical, and thermal properties of PUs. One of the fundamental reactions in synthesis of different polyurethanes is mainly reaction between diisocyanates and diols, which occurs in presence of catalysts and chain initiators. Polyurethane mostly consists of di- and poly-isocyanates as well as di- or polyhydroxy chemicals. It is also possible to use active hydrogen molecules that are not hydroxyl-based, such as those with the functional groups -SH, -NH2, and other active hydrogen groups. Practical considerations have primarily limited the usage of aliphatic amino groups in restricted chain extenders because they react with isocyanates too quickly. The major raw materials for these polymers are; isocyanate compounds, polyols and catalysts. Reactive hydroxyl-containing substances that typically have two or more reactive hydroxyl groups on the molecule are referred to as polyols. There is a large selection of these materials available for polyurethanes. IPNs are at least two or more partially interlaced polymer network but not covalently bonded and without breaking bond separation of network is not possible [1-9]. Materials classified as ferrites usually contain ferric oxide (Fe_2O_3) as one of their constituent elements. The four primary crystal forms of ferrites that can already studied and reported are hexaferrite or magneto plumbite (hexagonal structure), spinel ferrite (fcc structure), garnet (bcc structure), ortho ferrite (orthorhombic structure). Ferrites have drawn a lot of attention recently because of their outstanding magnetic properties, their use in permanent magnets and other technological applications. Ferrites particularly Hexaferrites and spinel have been widely employed in telecommunication for purposes to reduce microwave pollution brought on by ubiquitous wireless communication in wide range. Over the past few decades, spinel ferrites have

been an important component of ferromagnetic materials due to their exceptional magnetic properties, especially in radio frequency region, high electrical resistivity, mechanical hardness, and chemical stability [10-12]. Because of spinel ferrites' remarkable magnetic properties, particularly in radio frequency range they have played a significant role in in various industrial applications such as microwave absorption etc. The main issue with polyurethane is Low hydroxyl number which results in low tensile strength because its structural irregularity due of steric hindrance caused by long dangling fatty acid chains, sluggish secondary hydroxyl group curing, and a fundamentally low elastic modulus.
In order to encounter above mentioned problems of polyurethane, crossed linked networks are created by combining oil-based polyurethane with other polymers like styrene and methacrylate etc. which also known as interpenetrating polymer network. These IPN includes broad range of distinct polymer blend materials wherein at least one polymer exhibits cross-linking concurrently in presence of other.
In present paper, thermal, mechanical, dielectric and magnetic properties of thin flexible mat of $NiFe_2O_4$ and IPN of PU/PS have been reported. The ferrite ($NiFe_2O_4$) has been synthesized using Auto-Combustion method whereas flexible mats of prepared in-situ polymerization. Sintered powder of ferrite has been mixed in matrix of IPN of polyurethane and polystyrene during in-situ polymerization in presence of chain initiator and catalyst to make flexible sheets. The structural, microstructural, elemental confirmation as well as elemental distribution have also be studied.

EXPERIMENTAL METHODOLOGY

$NiFe_2O_4$ nanoparticles were synthesized using Auto Combustion method. During Auto-Combustion method, First, Metal Nitrates (Nickel Nitrate & Iron Nitrate) weighed in 1:1 stoichiometric proportion were separately dissolved in double distilled ionized water (DDI). The solutions of water dissolved nitrate were mixed with each by pouring slowly one in another along with citric acid as fuel agent for combustion process. The mixed solution was heated along with continuous stirring till powder formation. Liquid ammonia was used to maintain pH value of ~7 to ~8 during reaction. The dried powder was calcined at 700°C for 8 hours for phase formation. The calcined powder was mixed with polyvinyl alcohol as binder and pressed into circular discs using die and hydraulic press, followed by sintering at 1250°C for 2 hours. The sintered discs were again crushed into powder for sheets preparations. During In-situ polymerization for making thin sheets of IPN (Interpenetrating Polymer Network) of Polyurethane (PU) and Polystyrene (PS), $NiFe_2O_4$ along with chain initiator and catalyst used. Polyurethane was polymerized using Castor oil and MDI (Methyl Diisocyanate) in 1:1 equivalent weight. The ferrite powder was dispersed during high shear homogenizer and ultra-sonication. Following this, styrene was used as monomer for in-situ polymerization while preparation of sheets. Benzoyl peroxide (As Chain Initiator) and N, N dimethyl aniline (as a catalyst) has been used for IPN (Interpenetrating Polymer Network) sheet of $NiFe_2O_4$-PU/PS (5% & 10% wt of $NiFe_2O_4$). The X-ray diffraction technique was used for confirmation of $NiFe_2O_4$ phase in PU/PS matrix, whereas elemental confirmation was done using energy dispersive X-ray spectroscopy. Microstructural analysis has been carried out using scanning electron microscopy. Magnetic properties are studied using vibrating sample magnetometer (VSM). Thermo-Gravimetric analysis is used to study decomposition behavior of sheets which helps to study the effect of $NiFe_2O_4$ dispersion on weight loss of IPN. The tensile strength and elongation at break have been studied using Instron 30 (Tensile Strength analyzer) whereas impedance analyzer used to study dielectric properties.

RESULTS & DISCUSSION

X-ray diffraction data of $NiFe_2O_4$-PU/PS IPN sheet ($NiFe_2O_4$ & 10% wt. of $NiFe_2O_4$) is shown in figure 1. Since PU/PS is cross linking polymer network of Polyurethane (PU) and Polystyrene (PS) but sheets of $NiFe_2O_4$ incorporated PU/PS IPN represent uniformly dispersed $NiFe_2O_4$ in above mentioned wt% with IPN. Presence of $NiFe_2O_4$ in matrix of PU/PS interpenetrating polymer network is confirmed by diffraction peak at 2θ ~35.6° whereas broad peak from 2θ ~10°-20° reveals successful preparation of PU/PS IPN. To study structural formation of $NiFe_2O_4$ nanoparticles, diffraction pattern matched with JCPDS which represent structural information of $NiFe_2O_4$. All the diffraction peaks indexed according to JCPDS card no.01-1121 which gives information of F3dm space group No. 227. The maximum intensity diffraction peaks corresponding to 2θ ~ 35.6° in Fig. 1(a) and 1(b) represent F3dm space group No. 227 of $NiFe_2O_4$ as reported in JCPDS card no.01-1121.

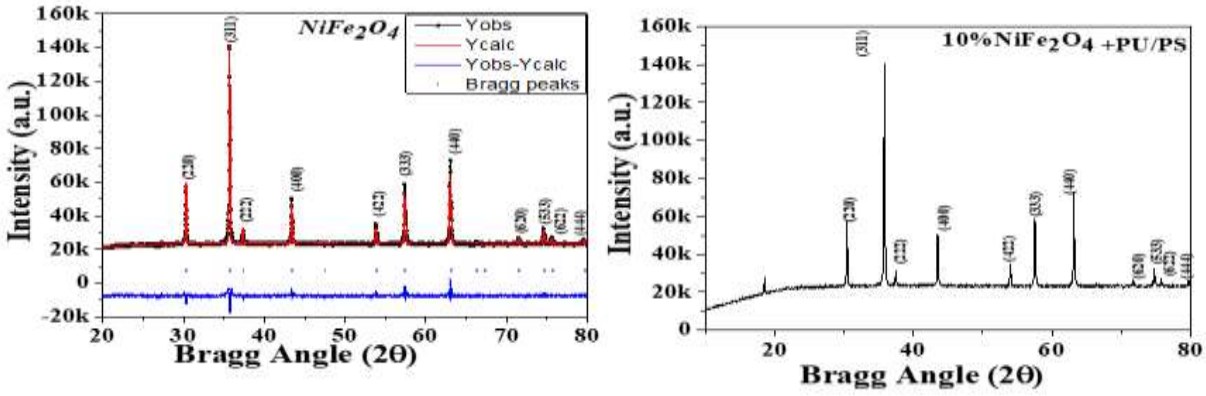

Figure 1: X-ray diffraction of Pristine $NiFe_2O_4$ & flexible mats of PU/PS IPN & $NiFe_2O_4$ (10%) incorporated in matrix of PU/PS IPN

To retrieve detailed structural information of $NiFe_2O_4$ nanoparticles, reitveld refinement of collected X-ray diffraction data has been carried out using full prof suite software. The required necessary parameters used during refinement such as lattice parameters, cell volume, atomic position have been taken from JCPDS card no.01-1121 & Tiwari et al. The background of experimentally collected data has been fitted using a sixth order polynomial whereas scale factor, zero displacement, lattice parameters, atomic position of Ni, Fe and O were taken as refinement parameters. Thompson Cox Hastings function with axial divergence symmetry was used to model peak profiles. The experimentally collected data matched quiet well with refined data (also shown in figure. 1). The refined lattice parameters & R-factors along with cell volume tabled in table 1 whereas atomic position of various atoms, and space group information given in table 2.

Table 1: Summarized refined cell parameters including lattice parameters, cell volume and R-factor, volume, Rietveld parameters for $NiFe_2O_4$

Atomic Position	***x***	***y***	***z***	**Space Group**
Ni	0.625	0.625	0.625	**F d 3 m No. 227**
Fe1	0.625	0.625	0.625	**Laue Class and Point Group: m-3m**
Fe2	0	0	0	
O	0.314	0.314	0.314	**Crystal System: Cubic**

Thermogravimetric analysis (TGA) under N_2 atmosphere has been carried out to study effect of dispersion of ferrite nanoparticles ($NiFe_2O_4$) on decomposition of flexible sheets of $NiFe_2O_4$ (10% wt) incorporated PU/PS IPN and PU/PS IPN. The TG (mg) vs. Temperature (K) of $NiFe_2O_4$ (5% & 10% wt)-PU/PS IPN is shown in figure 2. It is seen that initially weight loss (mg) is stable with increasing temperature upto ~549K and afterwards decreases with further increase in temperature showing decomposing behavior of IPN. The initial behavior of weight loss corresponds to stability of IPN against temperature. Graphs clearly manifests that dispersion of $NiFe_2O_4$ slightly improves decomposing efficiency against temperature which further enhances with increasing $NiFe_2O_4$ content. The weight loss (mg) stability extends from ~549K to ~567K as concentration of $NiFe_2O_4$ filler increases to 10 wt%. This aftereffect of incorporation of filler ($NiFe_2O_4$ incorporated) in matrix of matrix of PU/PS IPN known as labyrinth (barrier) effect generated by highly anisotropic oxide which results in delays escape of volatile degradation products from $NiFe_2O_4$ incorporated in matrix of PU/PS IPN.

Table 2: Summarized refined cell atomic position and space group information for $NiFe_2O_4$

Composition	**a[Å]**	**b[Å]**	**c[Å]**	**Cell Volume**	**R_p**	**R_{wp}**	**R_e**	**χ^2**
x = 0.02	8.3390	8.3390	8.3390	579.88	5.76	11.2	6.62	2.4

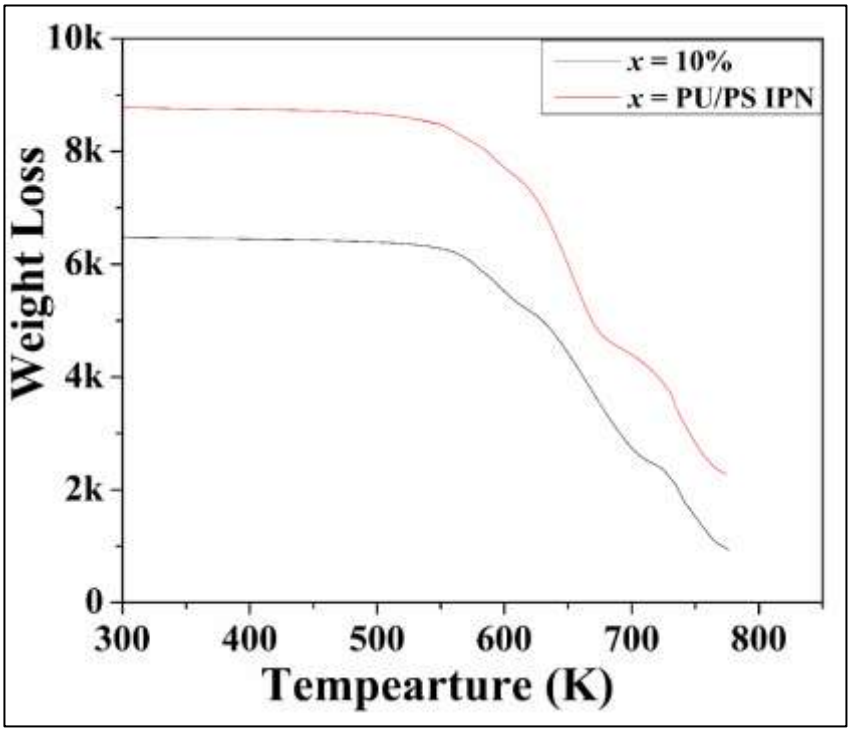

Figure 2: Temperature Dependence profile of Pristine PU/PS IPN & flexible mats of PU/PS IPN & $NiFe_2O_4$ (10%) incorporated in matrix of PU/PS IPN

FTIR spectra of $NiFe_2O_4$-PU/PS IPN sheet (PU/PS IPN &10% wt. of $NiFe_2O_4$) is shown in Figure 3. The transmittance peak at wave no. ~3322 cm^{-1} corresponds to Si-OH & OH stretching, whereas asymmetric and symmetric vibrations of methylene group (CH_2) in aliphatic carbon chain results from transmittance peaks at wave no. of ~2922 & 2850 cm^{-1}. The transmittance peaks corresponds to wave number ~1362 to 1181 cm^{-1} and ~1752 to 1732 cm^{-1} reveals presence of C-N

stretching and free urethane carbonyl C=O stretching vibrations. The transmittance bands at ~1039-1052cm^{-1} shows presence of Si-O-Si stretching. The transmission peak at ~673cm^{-1} represents stretching vibrations of metal oxide in octahedral group complex of Ni(II)-O^{2-} and Ni(III) Tetrahedral group complex of $NiFe_2O_4$ which further confirms the presence of spinel ferrite. Apart from this transmission peak at ~400 & 600cm^{-1} responsible for intrinsic stretching whereas peaks at wave numbers ~435, ~439, ~438 cm^{-1} may be due to octahedral complexes. The presence tetrahedral complexes in compound may be confirmed from peaks at ~601, ~613, ~599 & ~600 cm^{-1}. The presence of O-H stretching has been confirmed from transmittance peak appears at ~3388 cm^{-1} whereas ~1450 cm^{-1} & ~1647 cm^{-1}shows asymmetric stretching vibration of NO3 and carbo-oxalate anions. The transmittance band at ~2352 cm^{-1} appears due to stretching vibration of hydroxyl group in nanoferrites [10, 13-17]. The transmittance peaks in FTIR spectra directly stamped for presence of $NiFe_2O_4$ in PU/PS IPN sheets. Therefore it can be concluded that FTIR spectra directly endorsed X-ray diffraction data.

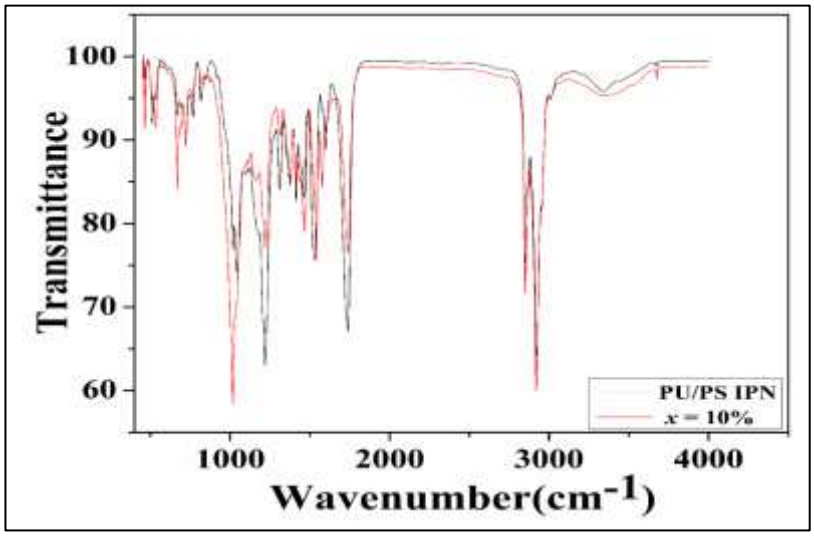

Figure 3: FTIR Spectra of Pristine PU/PS IPN & flexible mats of PU/PS IPN & $NiFe_2O_4$ (10%) incorporated in matrix of PU/PS IPN

Scanning Electron Micrographs of $NiFe_2O_4$-PU/PS IPN sheet (5% & 10% wt. of $NiFe_2O_4$) have been shown in figure 4. All the microstructure were recorded at same magnification and accelerating voltage of 10 kV using InLens detector for grain size as well as grain growth comparison. Grain like structures are clearly visualized in SEM micrographs. Uniform dispersion of ferrite particles in matrix of PU/PS IPN is confirmed by non- identical (both in shape and size) cross linked grains along with some porous structures.

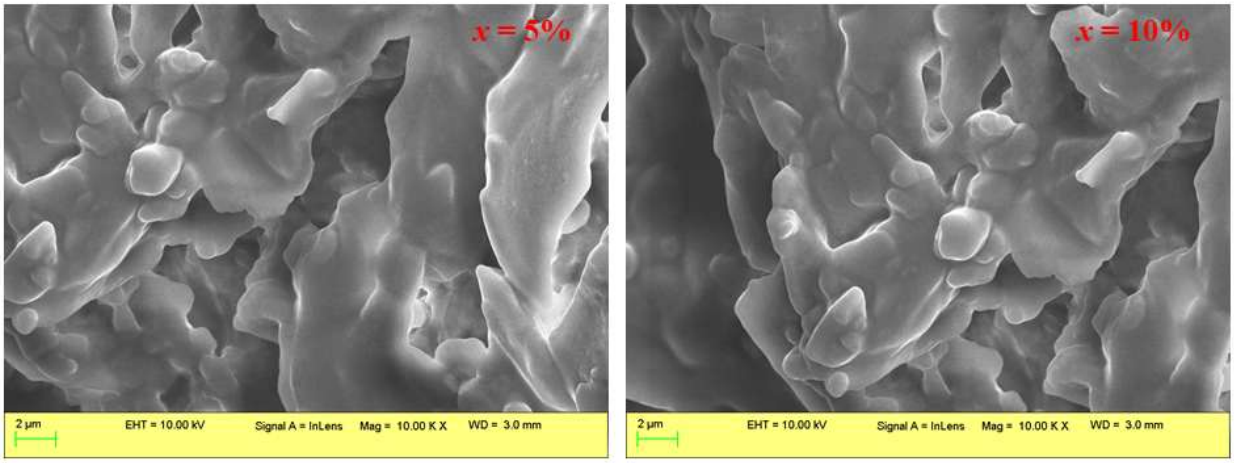

Figure 4: SEM Micrographs of Pristine PU & flexible mats of PU/PS IPN & with $NiFe_2O_4$ as filler (5 & 10%)

To further verify the elemental confirmation in flexible mats of $NiFe_2O_4$ incorporated PU/PS IPN, energy dispersive X-ray spectroscopy has been carried out. The peaks position of X-rays in EDS micrographs shown in figure 5 represent energies of X-rays generated from particular elements as per their respective binding energies. The elements according to their respective binding energies are shown in EDS micrographs. The elemental composition in terms of their wt% & mol% as obtained from EDS study is listed in table results obtained from this study also listed along with table of figure

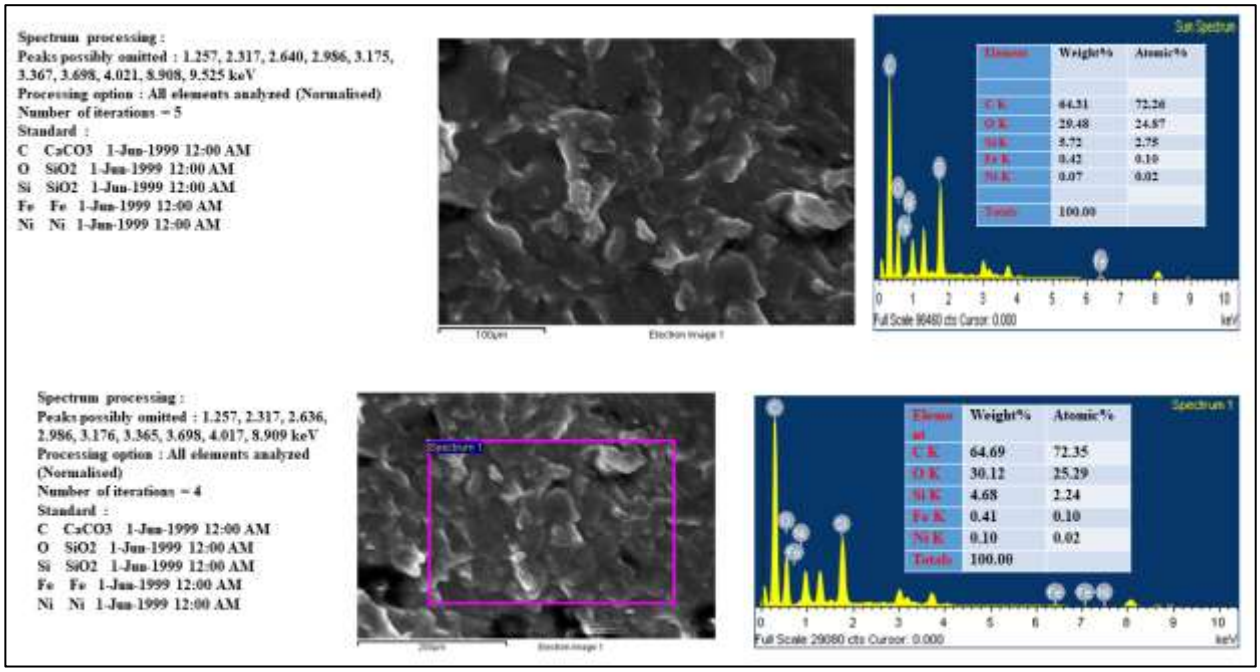

Figure 5: EDS Micrographs and Tables of flexible mats of PU/PS IPN & with $NiFe_2O_4$ as filler (5 & 10%)

Further, elemental distribution in flexible mats of $NiFe_2O_4$ incorporated PU/PS IPN has been studied from elemental mapping analysis shown in figure 6. Different colors have been assigned to different metal elements across selected scanning area during this measurement. The mapped micrographs directly evident for distribution of all elements which confirmed by energy dispersive x-ray spectra. The appearance of all colors in single micrograph proclaimed about presence of elements present according to EDS spectroscopy in selected scanned area whereas single color micrograph shows density of individual element present.

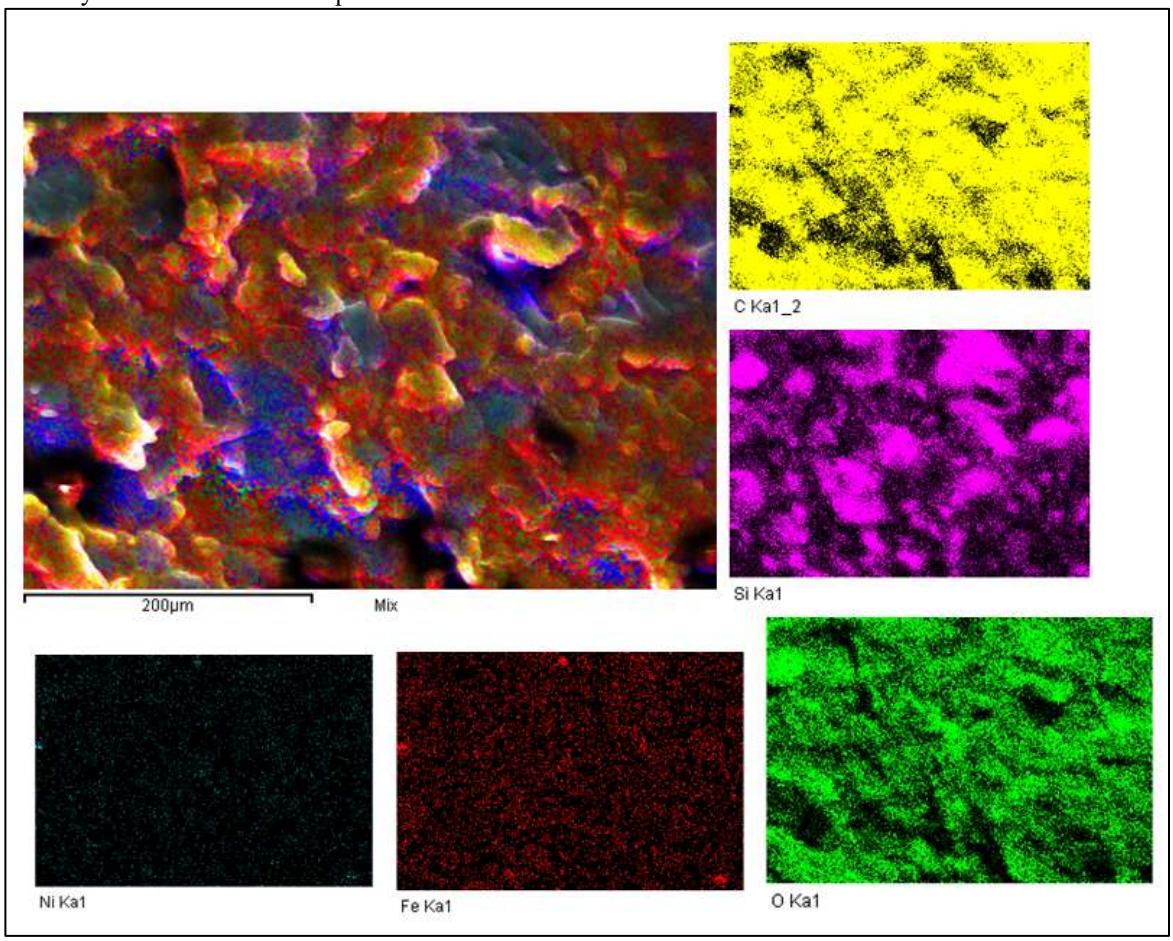

Figure 6: Elemental Micrographs of flexible mats of PU/PS IPN & with $NiFe_2O_4$ as filler (10%)

Magnetization vs. Magnetic Field hysteresis at room temperature of prepared $NiFe_2O_4$-PU/PS IPN sheets (PU/PS, 5% & 10% wt. of $NiFe_2O_4$) are shown in figure 7. Saturated hysteresis loops are observed for sheets of $NiFe_2O_4$-PU/PS IPN

which manifests presence of magnetic ordering whereas non-magnetic behavior of PU/PS shown by linearly varied magnetization w.r.t. magnetic field in 2nd & 3rd quaradrent. Such magnetic behavior of sheets results due to uniform dispersion of highly magnetic $NiFe_2O_4$ particles in non-magnetic PU/PS IPN matrix. It has been clearly visualized from graphs that M_r (Remnant Magnetization) as well as H_c (Coercive Field) in sheets decreased when compared with NiFe2O4 from because of non-magnetic behavior of IPN. The M_r (Remnant Magnetization) of sheets of $NiFe_2O_4$-PU/PS IPN has been continuously increases from 0.525 emu/g to 1.617 emu/g as concentration of ferrite ($NiFe_2O_4$) has been increased from 5% wt to 10% wt in PU/PS IPN sheets whereas coercivity decreases from 55.10 Oe to 48.08 Oe as concentration of $NiFe_2O_4$ increased 5% wt to 10% wt in PU/PS IPN. Since crystalline structure of $NiFe_2O_4$ is inverse spinel, and its net magnetization originates from the interaction of Fe3þ ions spinning in both tetrahedral and octahedral sites with Ni2þ ions in octahedric sites. Thus, at its magnetic saturation value, a net moment of 2 mB per molecule of NiFe2O4 would be anticipated [10, 12].

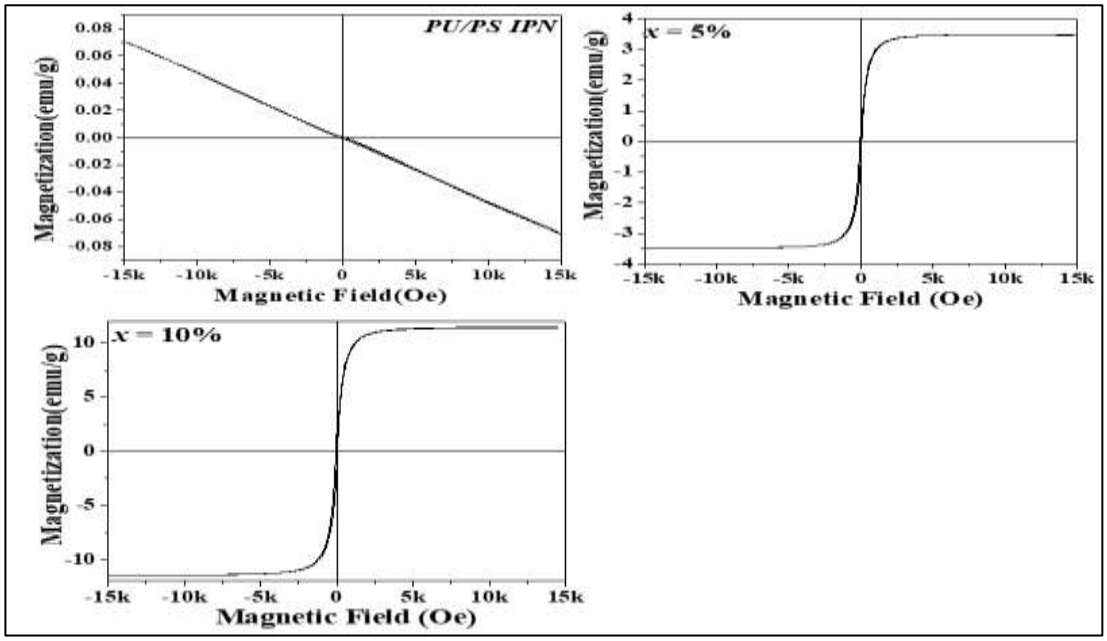

Figure 7: Magnetization (emu/g) vs. Applied Magnetic Field (Oe) $NiFe_2O_4$ & flexible mats of PU/PS IPN & with $NiFe_2O_4$ as filler (5% & 10%) & PU/PS IPN

Effect of ferrite nanoparticles on mechanical properties of PU/PS Interpenetrating polymer network is studied by recording the tensile strength and elongation at break and hardness of $NiFe_2O_4$ (5% & 10% wt)-PU/PS IPN sheets at a speed of 51 RPM. The measured values of tensile strength and elongation at break are listed in table 3. An increasing trend of elongation at break is observed with increase in $NiFe_2O_4$ filler concentration. The reason for increase in elongation at break may results due to exfoliation of ceramic filler used in nanocomposites. Moreover, chain interconnectivity generated by ceramic filler enhances the chain interconnectivity.

x	**Thickness (mm)**	**Elongation at Break (%)**	**Tensile Strength at beak (KG/Cm^2)**
PU/PS	**2.3**	**61.8**	**6.08**
5%	**1.50**	**56.59**	**9.55**
10%	**1.70**	**82.68**	**2.62**

Table 3: Elongation at Break, Tensile Strength and thickness of sheets of $CoFe_2O_4$ (5% & 10% wt)-PU/PS IPN

Room temperature dielectric properties (ε' & ε" vs. Frequency) of $NiFe_2O_4$-PU/PS IPN sheets (5% & 10% wt. of $NiFe_2O_4$) have been investigated and shown in figure 8. Figure 8 shows variation of ε' and ε" vs. Frequency (Hz). It has been clearly depicted from graphs that in lower frequency regime (<1 kHz), both ε' & ε" shows strong frequency dependent response and decrease as frequency increases in larger frequency regime. The overall dielectric constant (ε') is contributed by four types of polarizations namely dipolar, electronic, ionic and space charge polarization. Among these electronic and ionic polarizations possess very small relaxation time and hence contribute towards dielectric constant even at very high frequency. But, relaxation time of dipolar and space charge polarization is comparatively large. Hence, these polarizations cannot respond to frequent as polarity of applied signal changes in high frequency regime. As a result, in high frequency range, only ionic and electronic polarizations are effective, which give rise to as observed ordinary dielectric behavior explained by Jonhcher et al. [18-21]. Further it is observed that value of both ε' & ε" get enhanced as compared to pristine PU/PS IPN. It may be due to dielectric contribution of uniformly dispersed $NiFe_2O_4$. It has been clearly seen in graphs that as concentration of $NiFe_2O_4$ increases, value of both ε' & ε" increases reveals in modification in dielectric properties of PU/PS IPN by incorporation of $NiFe_2O_4$ in matrix of PU/PS IPN.

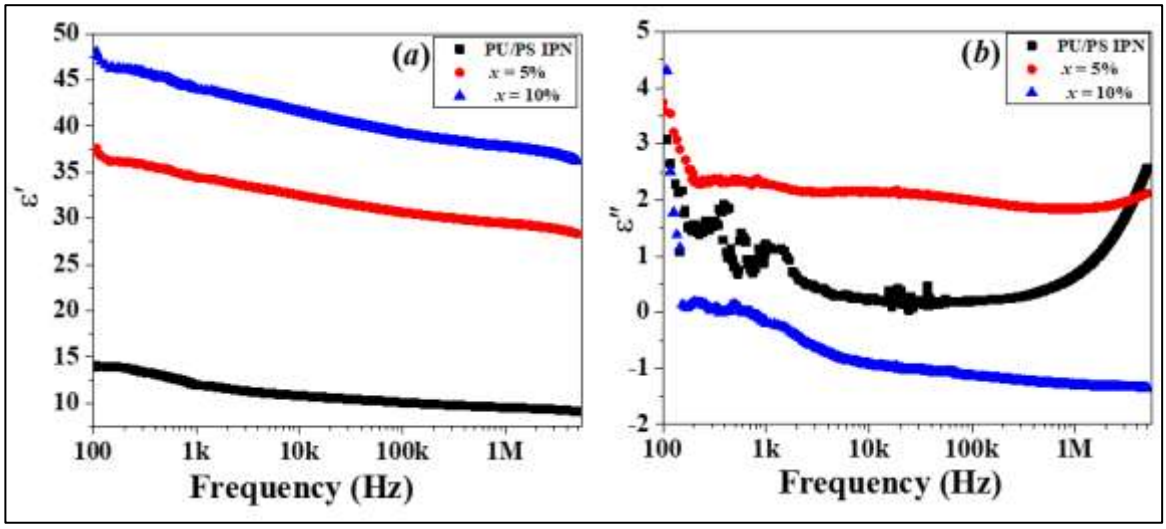

Figure 8: ε' & ε'' vs. Frequency (At Room Temperature) of Pristine PU/PS IPN & flexible mats of PU/PS IPN & with $NiFe_2O_4$ as filler (5 & 10%)

Room temperature σ_{ac} vs. Frequency (Hz) profile of $NiFe_2O_4$-PU/PS IPN sheets (5% & 10% wt. of $NiFe_2O_4$) is shown in figure 9. The σ_{ac} has been calculated from experimental dielectric data using formula: [22]

$\sigma_{ac} = 2\pi f \varepsilon' \varepsilon_o \tan\delta$

Where f, tanδ , ε' & ε'' are frequency, dielectric loss, real and imaginary part of dielectric permittivity respectively. The observed variation of σ_{ac} vs. Frequency consists two regimes. σ_{ac} is almost independent of frequency in the range 100 Hz to 100 kHz and afterwards linearly increases with increase in frequency. The frequency independent part of conductivity is termed as dc conductivity (σ_{dc}) whereas frequency dependent part is known as ac conductivity (σ_{ac}). The conductivity profile can be generally analyzed using Jonscher's power law: [23]

$\sigma_{ac} = \sigma_{dc} + A\omega^n$

Where σ_{ac} = ac conductivity, σ_{dc} = dc conductivity, A = dispersion parameter representing the strength of Polarizability & "n" is dimensionless parameter which gives information about interaction between mobile ions with the lattice in which they interact [22-23].

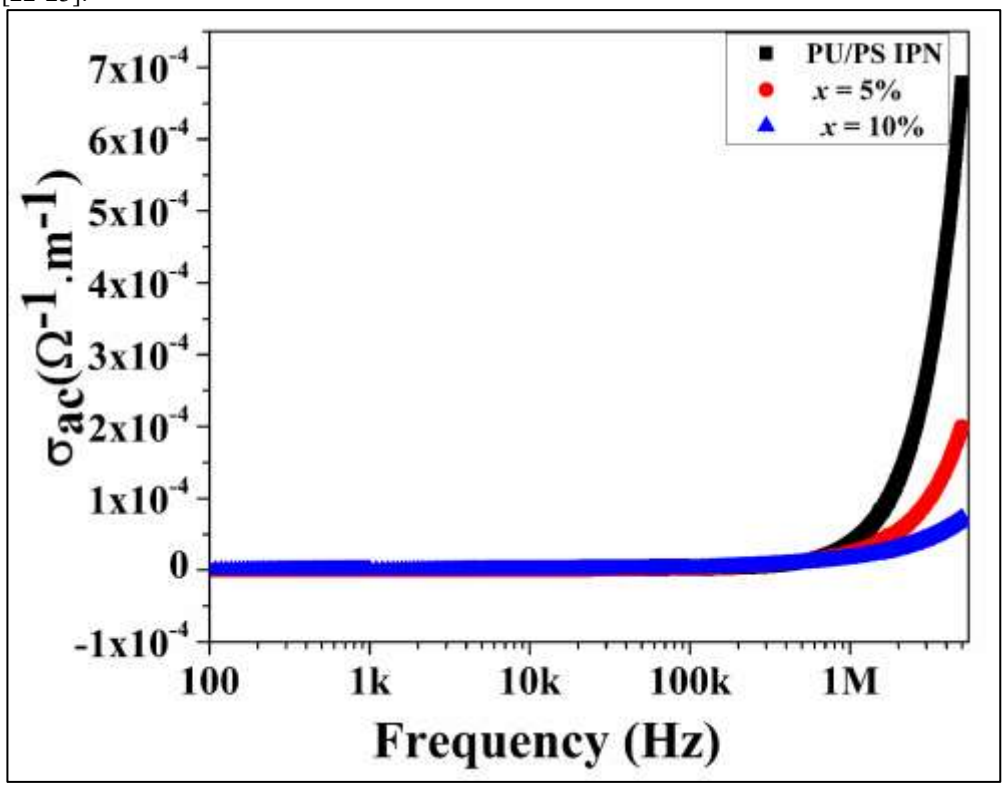

Figure 9: σ_{ac} vs. Frequency (At Room Temperature) of Pristine PU/PS IPN & flexible mats of PU/PS IPN & with $NiFe_2O_4$ as filler (5 & 10%)

CONCLUSION

Flexible Sheets of PU/PS IPN-$NiFe_2O_4$ has been successfully prepared using In-situ polymerization PU/OS along with $NiFe_2O_4$ as filler in presence of catalyst and chain initiator. The X-ray diffraction data as well as FTIR spectra confirms presence of $CoFe_2O_4$ in matrix of IPN. The Thermal gravimetric data shows improvement in weight loss against

temperature incorporation of filler ($NiFe_2O_4$ incorporated) in matrix of matrix of PU/PS IPN known as labyrinth (barrier) effect generated by highly anisotropic oxide which results in delays escape of volatile degradation products. The confirmation and uniform distribution of elements has been confirmed from Energy Dispersive and elemental mapping spectroscopy. The magnetic hysteresis in non-magnetic PU/PS also confirms presence $NiFe_2O_4$ as filler in PU/PS matrix and magnetization increases with increasing $CoFe_2O_4$ content. The enhancement in dielectric properties also results due to presence of $CoFe_2O_4$ in matrix of PU/PS IPN. The increment in elongation at beak directly reveals enhancement in mechanical properties with simultaneous magnetic behavior of PU/PS incorporated with magnetic ceramic ($NiFe_2O_4$) and may be due to interaction of Fe3þ ions spinning in both tetrahedral and octahedral sites with Ni2þ ions in octahedric sites.

REFERENCES

1. Król, P., *Generalization of kinetics in the reaction of isocyanates and polyols for modeling a process-yielding linear polyurethane, 1.* Journal of Applied Polymer Science, 1995. **57**(6): p. 739-749.
2. Kong, X. and S.S. Narine, *Physical Properties of Polyurethane Plastic Sheets Produced from Polyols from Canola Oil.* Biomacromolecules, 2007. **8**(7): p. 2203-2209.
3. Frisch, K.C. and L.P. Rumao, *Catalysis in Isocyanate Reactions.* Journal of Macromolecular Science, Part C: Polymer Reviews, 1970. **5**(1): p. 103-149.
4. Oprea, S., *Synthesis and Properties of Polyurethane Elastomers with Castor Oil as Crosslinker.* Journal of the American Oil Chemists' Society. **87**(3): p. 313-320.
5. Zilg, C., Thomann, R., Mülhaupt, R., and Finter, J.,, *Polyurethane nanocomposites containing laminated anisotropic nanoparticles derived from organophilic layered silicates.* Advanced Materials, 1999. **11**(1): p. 49-52.
6. Frisch, K.C., S.L. Reegen, and B. Thir, Kinetics of alcohol and polyether polyol-isocyanate reactions using metal catalysts. Journal of Polymer Science Part C: Polymer Symposia, 1967. **16**(4): p. 2191-2201.
7. Narine, S., et al., Physical Properties of Polyurethanes Produced from Polyols from Seed Oils: I. Elastomers. Journal of the American Oil Chemists' Society, 2007. **84**(1): p. 55-63.
8. Lligadas, G., et al., Polyurethane Networks from Fatty-Acid-Based Aromatic Triols:â€‰ Synthesis and Characterization. Biomacromolecules, 2007. **8**(6): p. 1858-1864.
9. Oprea, S., Synthesis and Properties of Polyurethane Elastomers with Castor Oil as Crosslinker. Journal of the American Oil Chemists' Society. **87**(3): p. 313-320.
10. Rashmi Tiwaria , Manojit Dea, H.S. Tewaria, S.K. Ghoshal, Structural and magnetic properties of tailored $NiFe_2O_4$ nanostructures synthesized using auto-combustion method, Results in Physics, 16 (2020) 102916
11. E. C. Snelling " Soft Ferrites, Properties and Applications". Butterworth and Co. (Publishers) Ltd. London (1988).
12. J.G.S. Duquea , E.A. Souzaa, C.T. Menesesa, L. Kubota, Magnetic properties of $NiFe_2O_4$ nanoparticles produced by a new chemical method, Physica B 398 (2007) 287–290
13. Nayak, P. and B. Singh, Instrumental characterization of clay by XRF, XRD and FTIR.
14. Bulletin of Materials Science, 2007. **30**(3): p. 235-238.
15. Kaushik, A., Ahuja, D. and Salwaani, V., Synthesis and Characterization of the organically modified clay/castor oil based chain extended polyurethane nanocomposites, Composite, 2011 42: 1534-1541.
16. Xue, S.C., Zhang, Z.P. and Ying, S.K., Reaction Kinetics of Polyurethane/Polystyrene Interpenetrating Polymer network by Infra-Red Spectroscopy. Polymer, 1989, 30 (7), 1269-1274.
17. Habibi, M.H. and Parhizkar, H.J., FTIR and UV-VIS diffuse reflectance spectroscopy studies of the wet chemical (WC) route synthesized nano-structure CoFe2O4 from CoCl2 and FeCl3, Spectrochimica Acta Part A: Molecular and biomolecular Spectroscopy 2014, 127, 102-106.
18. Kumar M, Yadav KL. J. Phys.: Condens. Matter. 2002;19:242202.
19. Cole KS, Robert H. Dispersion and Absorption in Dielectrics:- Alternating Current Characteristics. Journal of Chemical Physics. 1941;9:341–351.
20. Havriliak S, Negami S. A complex plane representation of dielectric and mechanical relaxation processes in some polymers. Polymer. 1967;8:161-210. DOI: 10.1016/0032-3861 (1967) 90021-3.
21. Prakash V, Choudhary SN, Sinha TP. Dielectric relaxation in complex perovskite oxide BaCo1/2W1/2O3. Physica B. 2008;403:103–108.
22. Jonscher AK. The Universal dielectric response. Nature. 1977;267:673-679.
23. Pradhan DK, Behera B, Das PR. Studies of dielectric and electrical properties of a new type of complex tungsten bronze electroceramics. J. Mater. Sci. Mater. Electron. 2012;23:779.